Dynamics of collapsing multi-bubble arrangements

T. Hopfes[1]*, Z. Wang[1], M. Giglmaier[1] and N. A. Adams[1]

[1]Institute of Aerodynamics and Fluid Mechanics, Technical University of Munich,

Boltzmannstr. 15, D-85748 Garching bei München, Germany

*thomas.hopfes@tum.de

Abstract

A planar shock front produced in a shock tube provides an instantaneous pressure rise within a water-like gelatin mixture that contains arrangements of millimeter-sized air bubbles. This article studies how bubbles react to this sudden pressure jump and analyzes the complex dynamics and interactions that are involved. Bubble dynamics are captured with a high-speed camera and extracted image sequences for conducted experiments are presented. Experiments include pairs of bubbles of equal and different size in the free field as well as near a solid boundary. For equally sized bubbles in the free field we observe jetting toward each other and coalescence after the second oscillation cycle. Bubbles of different size show a combination of jetting toward and jetting away caused by the out-of-phase oscillation. For a bubble pair aligned normal to a solid boundary we observe that the outer bubble influences the collapse of the inner bubble so that there is no aspherical behavior or jet development. An exemplary experiment with three bubbles in a triangular arrangement next to a solid boundary is presented to highlight the potential for future investigations.

1 Introduction

Collapsing bubbles play an important role in many medical applications such as shock wave lithotripsy, targeted drug delivery or sonothrombolysis (Unger *et al.*, 2004). Lithotripsy, for example, is an established medical procedure to non-invasively destroy gallstones in the human body by focusing extracorporeally generated shock waves on the target (Chaussy, Brendel and Schmiedt, 1980). Cavitation bubbles are formed in the liquid by a focused tensile wave that follows the preceding shock wave. An aspherical collapse of these bubbles then leads to strong erosive effects through liquid jets and shock wave emission and hence transient cavitation is the dominant mechanism that strongly determines the overall effectiveness (Coleman and Saunders, 1993). The idea behind targeted drug delivery is to use coated microbubbles as drug carriers in the human body. Ligands on the bubble surface target specific cells before ultrasound pressure pulses, generated outside the body, break the bubbles apart and release the carried drug. In both procedures multiple bubbles interact with each other as well as with boundaries like cells or human tissue. It is thus essential for improving the methods to have a good understanding of general bubble dynamics. To achieve that, often single bubbles are studied. But while a thorough analysis of a single bubble collapse is necessary for understanding the fundamentals, it is not a good representation of nature where bubbles are often present in clouds that interact significantly.

Literature shows elaborate research on the topic of multi-bubble interaction. Several studies investigate laser-induced bubble pairs, e.g. (Lauterborn and Hentschel, 1985; Tomita, Shima and Sato, 1990; Han *et al.*, 2015), while other experiments use spark-generated bubbles. Fong *et al.* (2009), for example, use this method to analyze the influence of phase difference on oscillating bubble pairs in the free field. Summarizing their own work and previous literature, they classify four types of collapse phenomena, namely catapult, coalescence, jet toward and jet away. Further research solidifies and expands this classification for bubbles of unequal size (Chew *et al.*, 2011; Han *et al.*, 2015). Apart from the studies of vapor bubbles, also gas bubbles are investigated. Using a two-dimensional gel technique Dear and

Field (1988) analyze, for example, the collapse of arrays of gas cavities under strong shock loading. Other research on gas bubbles is presented by Tomita, Shima and Ohno (1984) who collapse air bubbles that are carefully placed under a solid surface in bubble pairs or as parallel and concentric circular arrangements. Despite the existing research, there is a need for more experimental investigation on three-dimensional arrangements of multiple bubbles and particularly interesting could be to analyze differences in the behavior of gas bubbles in contrast to generated vapor bubbles. This topic is therefore studied experimentally and is discussed here by describing the experimental arrangement in section 2, studying different multi-bubble arrangements in section 3 and concluding the work in section 4.

2 Experimental setup

For the present work, a planar shock front formed in a shock tube provides an instantaneous pressure jump within a water-like gelatin. A schematic diagram of the experimental setup is shown in fig. 1. The shock tube, with an overall length of 22.5 m and an inner diameter of 290 mm, consists of three parts: the driver, the driven and the test section. A diaphragm separates the high-pressure driver section, used in this study at pressures of up to 8 bar, from the driven section at atmospheric pressure. After the diaphragm breaks, a shock wave forms and propagates toward the test section.

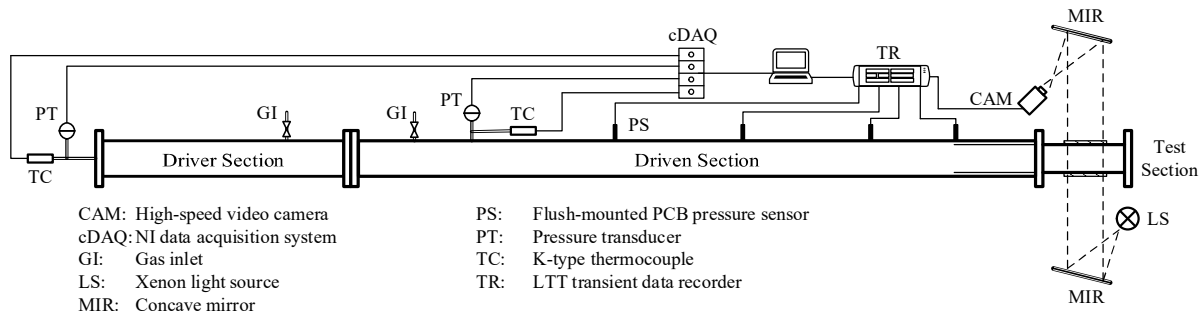| CAM:	High-speed video camera	PS:	Flush-mounted PCB pressure sensor
cDAQ:	NI data acquisition system	PT:	Pressure transducer
GI:	Gas inlet	TC:	K-type thermocouple
LS:	Xenon light source	TR:	LTT transient data recorder
MIR:	Concave mirror		

Figure 1: Sketch of the shock tube and connected systems.

Other researchers have also investigated bubble dynamics by means of a shock tube, e.g. (Fujikawa and Akamatsu, 1978; Vokurka, Beylich and Kleine, 1992), but the present study uses a different setup. Accordingly, fig. 2(a) shows the shock wave propagating into the test section filled with gelatin. The shock wave reflects almost ideally at the air-gelatin interface due to the high difference in acoustic impedance of the two materials. Since the pressure must be equal at the interface, a compression wave propagates into the gelatin. Bubbles are positioned in the gelatin near the end of the test section as shown exemplary in fig. 2(b-c) and rest under well-defined initial conditions, such as constant temperature, constant pressure and zero initial velocity.
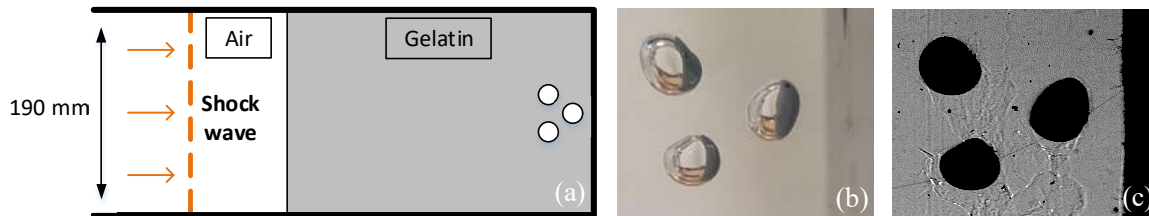

Figure 2: Experimental setup for bubble dynamics experiments (a), with an exemplary bubble arrangement shown as a direct photograph (b) and visualized with shadowgraph technique (c).

With the arrival and reflection of the compression wave, the ambient pressure around the bubbles rises instantaneously by several bars and this pressure change drives the bubble oscillation or bubble collapse. Ideally, the ambient conditions around the bubbles remain constant until the compression wave reflects as an expansion wave at the air-gelatin interface and returns to the bubble position, which for 400 mm gelatin gives a test time of around 0.5 ms.

In this setup, Gelrite^{TM} Gellan Gum for microbiological applications combined with magnesium sulfate is dissolved in distilled water to form a clear, agar-like gelatin. Within the gelatin, the bubbles are produced by carefully inserting the needle of a syringe and releasing a defined amount of air. Gelatin has already been used to investigate bubble dynamics, namely for the two-dimensional gel technique, e.g. (Dear and Field, 1988; Swantek and Austin, 2010), but is now applied in a three-dimensional setup. For visualization, we apply a Z-type schlieren system with a 150 W constant Xenon light source to create either schlieren images by cutting light at the second focal point or 'focused shadowgraph' images when no light is cut (Settles, 2001). Creating schlieren images is useful for shock visualization, but using the direct shadowgraph provides more light and thus allows a higher frame rate or more optical zoom. The optical system projects the visualized section along the line-of-sight on a camera focal plane and thus gives a two-dimensional representation of the three-dimensional bubble. The entire collapse procedure is recorded with a Shimadzu HyperVision HPV-X ultra-high-speed camera that produces videos of 128 consecutive frames with a resolution of 400x250 pixels at up to 5 million frames per second. Simultaneously, PCB Piezotronics ICP® fast-response pressure sensors, connected to a LTT transient recorder, monitor and record the pressure during the collapse at up to 16 locations at a frequency of 4 MHz per channel.

A new test section was designed to conduct the experiments according to the described method. Due to delays in deliveries and the manufacturing process, the section was completed only recently and now allows to conduct experiments according to the simplified sketch shown in fig. 2(a). First experiments have since shown the potential, but also show a slow pressure rise that leads to weak bubble oscillations instead of collapses. This effect is most likely caused by trapped air in gaps between component parts, but the limited time made it necessary to continue working with a preliminary setup that uses acrylic boxes filled with gelatin that are placed in the test section. This workaround allows to measure the pressure in the air surrounding the boxes, but not inside the gelatin. As another drawback, undesired effects like deformation of the acrylic box and additional wave motion within the surrounding gas of the box influence the experiments. The following preliminary results should thus be handled with care, but nevertheless show that the basic features of the concept work well and that a qualitative analysis is possible. New results without the mentioned uncertainties are expected soon.

3 Preliminary results

To characterize bubble pairs usually three non-dimensional parameters are defined: a relative distance, a size ratio and a phase difference. Fong *et al.* (2009) define the relative initial bubble distance, d', as

$$d' = d/(R_1 + R_2) \tag{1}$$

where d is the distance between the bubble centers and R_1 and R_2 are the initial radii of the two bubbles. After Chew *et al.* (2011) the size difference, S, is defined as

$$S = R_L/R_S \tag{2}$$

with R_L and R_S as the large and the small bubble respectively. The third parameter, $\Delta\theta$, indicates the phase difference of the two bubbles, but the definition cannot be transferred easily from the literature due to the different experimental setups. In this study, bubbles are initially present and thus no time difference of bubble nucleation exists. The definition of Chew *et al.* (2011) is simplified for the current case to

$$\Delta\theta = 1 - t_{osc,S}/t_{osc,L} \tag{3}$$

where t_{osc} gives an oscillation period, taken here as the time from maximum to minimum bubble radius in contrast to the duration from bubble nucleation to bubble collapse in the original definition. With the oscillation time of the smaller bubble, $t_{osc,S}$, being shorter than the oscillation time of the bigger bubble, $t_{osc,L}$, always a positive value for the phase difference results with 0 as the minimum for equally sized and equally oscillating bubbles. Taking the thought further, a linear relation between radius and collapse time is assumed here that can be justified by the Rayleigh collapse time for single bubbles (Brennen, 2005). This results in the phase difference solely depending on the size ratio and equation (3) transforming to

$$\Delta\theta = 1 - R_S/R_L = 1 - 1/S \tag{4}$$

This definition could overly simplify the relation but is applied here for a first assessment. With the help of the parameters, the collapse pattern for bubble pairs can be classified into four types defined as catapult, coalescence, jetting away and jetting toward. Using the presented setup, we conduct experiments on pairs of air bubbles, analyze the results qualitatively and try to classify the behavior according to the four types. Figure 3 shows two bubbles in the free field of almost equal size ($S \approx 1$, $\Delta\theta = 0$) in close proximity ($d' \approx 1.2$). Images 1 through 3 show the first contraction of both bubbles after the pressure increase and image 3 clearly depicts an asymmetric behavior of both bubbles. It can be assumed that a liquid jet develops in each bubble toward the other bubble respectively. This is indicated as both bubbles point toward each other on the close sides and develop an indentation on the far side, visible as a flattening (image 3). During the rebound (images 4 and 5) and second collapse (6 and 7) a jet is also clearly exiting the left bubble, reaching its maximum length in image 6. In addition, last images show that the overall motion of the bubbles, driven by the inertia of the liquid, is toward each other. Thus, this behavior fits the jetting toward type that is also expected for this set of parameters (Fong *et al.*, 2009; Chew *et al.*, 2011).
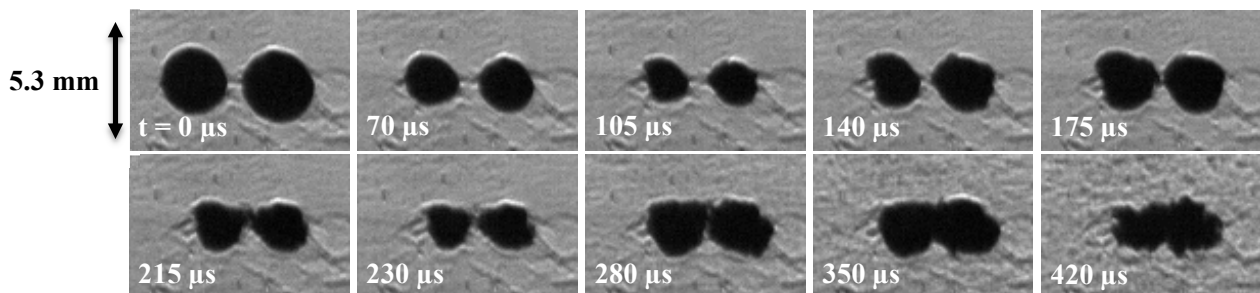

Figure 3: Two almost equally sized bubbles jet toward each other.

In the last two images of fig. 3 the two bubbles are not separated anymore, but merge into a single bubble that is also visible long after the experiment. In literature, the coalescence type is not observed for $d' > 1$, but the definition also refers only to the first oscillation cycle. Due to the different setup we can observe several cycles and here the experiment shows that the bubbles merge. Nevertheless, it is not feasible to compare this with the coalescence type directly, because after the first oscillation a big influence by other parameters like bubble motion and dynamics in the flow field must be taken into consideration.

Chew *et al.* (2011) extend the original classification to include differently sized bubbles and define regimes in graphs of size difference and relative distance against the phase difference. This classification can be compared to another conducted experiment of two differently sized bubbles ($S \approx 1.7$, $\Delta\theta = 0.42$) positioned very close to each other ($d' \approx 1.1$) in the free field (fig. 4). For this case, the set of parameters predicts a behavior in between the regime of both jetting away and jetting toward (Chew *et al.*, 2011).
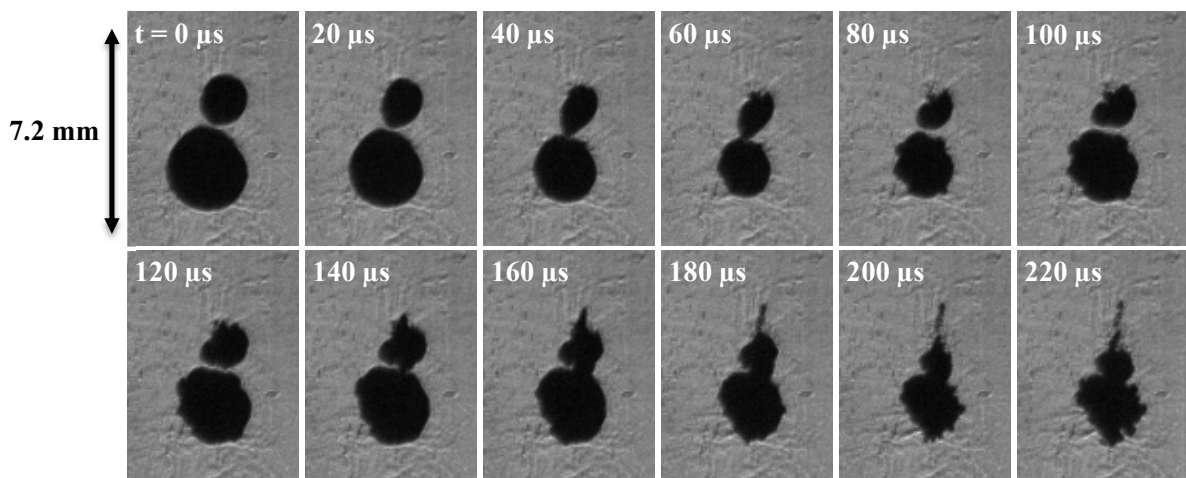

Figure 4: A bubble pair of different size shows mixes behavior of jetting away and jetting toward.

Initially, the small bubble elongates toward the big bubble during the first contraction. This could indicate jetting toward, but the following behavior does not confirm this classification. During the rebound and second collapse the small bubble develops a strong jet away from the bigger bubble which can be seen clearly as a thin propagating line from image 8 on. This contradicts the earlier classification and indicates jetting away, although the large bubble, as before, does not show any visible sign of jetting. In addition, despite some differences, there is also a resemblance of these combined effects to the catapult type which is otherwise only observed for induced bubbles with $d' < 1$ (Fong et al., 2009). Resembling features are the elongation toward and the strong jet development away from the second bubble, but other aspects are clearly different. Despite jetting away, the bulk of the small bubble slowly moves toward the big bubbles until they get into contact in the final images. This behavior of motion in opposing directions is similar to what Lauterborn and Hentschel (1985) observe for bubbles of a considerable size difference. In their case the small bubble divides into two parts and develops two jets in opposite directions. It remains therefore difficult to classify the behavior for the shown experiment according to the literature, for which the non-dimensional parameters would predict jetting away or toward. Neither of the two types fully matches the more complex behavior that is observed.

For many applications not only the interaction between bubbles, but the behavior near boundaries is interesting. It is well known that single bubbles collapse aspherically in the presence of a solid boundary, develop liquid jets toward the surface and emit shock waves that can cause severe erosion. It is thus interesting how systems of multiple bubbles near a solid boundary behave and how that interaction affects the erosion potential. Figure 5 depicts selected stages of a collapsing bubble pair of almost equal size ($S < 1.1$) arranged normal to a solid wall. The right bubble does not collapse aspherically, but rather remains at the same position during the primary collapse and the rebound. As already shown, the bubble wants to collapse toward the other bubble, but is also attracted by the solid boundary. For this experiment, the two effects offset, the bubble collapses spherically and remains at the initial position.

Figure 5: Collapsing gas bubble pair aligned normal to a solid wall.

The left bubble, however, is attracted by both the inner bubble and the solid wall and thus shows asymmetric behavior and collapses toward the right (image 3). This induced motion continues during the following rebound and the second collapse (images 4 to 6) and the bubbles move closer together. Being affected by the motion of the left bubble, also the bubble close to the wall deforms asymmetrically and motions toward the boundary (image 6). In summary, the outer bubble stops the inner bubble from collapsing aspherically during the first contraction which differs significantly from a single bubble collapse and results in a reduction of the bubble's damage potential. After that, a motion toward the surface is induced in following oscillations that further shows how the bubbles interact.
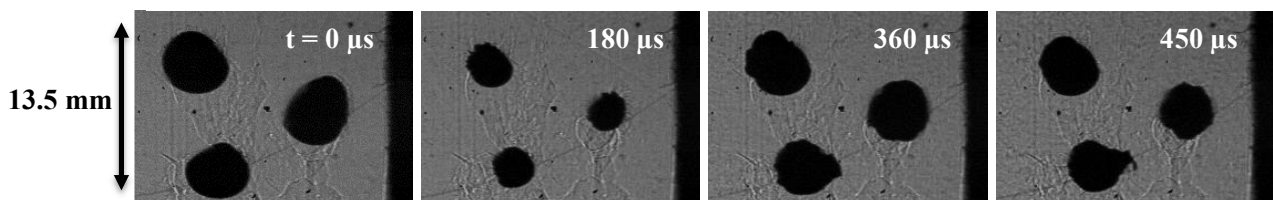

Figure 6: Three air bubbles in a triangle arrangement next to a solid boundary.

The presented experimental setup also allows to produce other configurations of multiple bubbles. An example of three bubbles in a triangle arrangement near a solid boundary is presented in fig. 6. Only a weak pressure increase was achieved in this experiment and consequently the collapse and the bubble interaction are not very pronounced here, which is why the results are not interpreted further.

4 Conclusion

We have applied a straight-forward experimental procedure to analyze the complex effects during the collapse of multi-bubble systems in the free field and near a solid boundary. The concept provides particularly homogeneous initial conditions and a single planar shock wave as collapse trigger to analyze the dynamic response. Despite mainly using a preliminary setup that causes undesired wave motion and did not allow for valid pressure measurements, the conducted experiments show delicate features of bubble-bubble and bubble-wall interaction. Comparing the observation with the literature shows both similarities and differences in how air bubbles, in contrast to induced vapor bubbles, behave and can be classified with the non-dimensional parameters. Especially the definition of the phase difference is difficult to interpret for our experimental setup, but an adaption can only be done after the observations are confirmed by more experiments in an improved experimental setup. Integrating our results into previous findings can then lead to a better understanding of the dynamics of multi-bubble systems, which is very important to improve medical applications like targeted drug delivery, in which bubbles play a significant role.

References

Brennen, C. E. (2005) *Fundamentals of Multiphase Flow*. Cambridge: Cambridge University Press.

Chaussy, C., Brendel, W. and Schmiedt, E. (1980) 'Extracorporeally induced destruction of kidney stones by shock waves.', *Lancet (London, England)*, 2(8207), pp. 1265–8.

Chew, L. W. *et al.* (2011) 'Interaction of two differently sized oscillating bubbles in a free field', *Physical Review E - Statistical, Nonlinear, and Soft Matter Physics*, 84(6).

Coleman, A. J. and Saunders, J. E. (1993) 'A review of the physical properties and biological effects of the high amplitude acoustic fields used in extracorporeal lithotripsy', *Ultrasonics*, 31(2), pp. 75–89.

Dear, J. P. and Field, J. E. (1988) 'A study of the collapse of arrays of cavities', *Journal of Fluid Mechanics*, 190, pp. 409–425.

Fong, S. W. *et al.* (2009) 'Interactions of multiple spark-generated bubbles with phase differences', *Experiments in Fluids*, 46(4), pp. 705–724.

Fujikawa, S. and Akamatsu, T. (1978) 'Experimental Investigations of Cavitation Bubble Collapse by a Water Tube', *Japan Society of Mechanical Engineers*, 21, pp. 223–230.

Han, B. *et al.* (2015) 'Dynamics of laser-induced bubble pairs', *Journal of Fluid Mechanics*, 771, pp. 706–742.

Lauterborn, W. and Hentschel, W. (1985) 'Cavitation bubble dynamics studied by high speed photography and holography: part one', *Ultrasonics*, 23(6), pp. 260–268.

Settles, G. S. (2001) *Schlieren and Shadowgraph Techniques*. Springer Berlin Heidelberg.

Swantek, A. B. and Austin, J. M. (2010) 'Collapse of void arrays under stress wave loading', *Journal of Fluid Mechanics*.

Tomita, Y., Shima, A. and Ohno, T. (1984) 'Collapse of multiple gas bubbles by a shock wave and induced impulsive pressure', *Journal of Applied Physics*, 56(125).

Tomita, Y., Shima, A. and Sato, K. (1990) 'Dynamic behavior of two-laser-induced bubbles in water', *Citation: Appl. Phys. Lett. Physics of Fluids Journal of Applied Physics*, 571(67), pp. 12103–3560.

Unger, E. C. *et al.* (2004) 'Therapeutic applications of lipid-coated microbubbles', *Advanced Drug Delivery Reviews*, pp. 1291–1314.

Vokurka, K., Beylich, A. E. and Kleine, H. (1992) 'Experimental study of gas bubble oscillations using a shock tube', *Acta Acustica united with Acustica*, 4, p. 268–275(8).